Journal of New Materials for Electrochemical Systems 15, 265-270 (2012)

High Surface Area Lithium Titanate Electrode for Li-ion Batteries

Nishant M. Tikekar[1], John J. Lannutti[1,*], Ramchandra Rao Revur[2] and Suvankar Sengupta[2]

[1]Department of Materials Science and Engineering, 448 MacQuigg Labs, 105 W Woodruff Avenue, Ohio State University, Columbus OH 43210, USA
[2]Metamateria Technologies, 1275 Kinnear Road, Columbus OH 43212, USA

Received: November 30, 2011, Accepted: January 09, 2012, Available online: April 11, 2012

Abstract: *A lithium titanate ($Li_4Ti_5O_{12}$) anode composed of submicron fibers with nanosize grains was fabricated by electrospinning from spin dopes prepared from nanoparticles of lithium titanium oxide ($Li_4Ti_5O_{12}$) and polyvinylpyrolidone (PVP) in a solvent. Optimal electrospinning conditions and solvent composition that could be electrospun into fibers under a variety of ambient conditions were determined. Pyrolyzing the electrospun fibers at high temperatures (700˚C for 5 hours in air) and plasma-treating in oxygen (500 mTorr for 30 m) revealed a nano-size grain structure within the individual fibers. Electrochemical testing with metallic lithium as a reference electrode displayed promising capacities for three charging cycles. The C rates displayed complete charging when the charging time was at least 10 minutes. However, faster charging resulted in a loss of capacity to as low as 50% when charged in less than three minutes. This degradation appears to be triggered by trace amounts of a secondary phase introduced by standard purity precursors used for preparing lithium titanate. Evidence for this was found using x-ray fluorescence revealing the presence of iron and silicon oxides.*

Keywords: Lithium titanate, Li-ion battery, Electrospinning, Surface area

1. INTRODUCTION

During the past two decades, the requirements for energy storage in both portable and static applications have increased tremendously. As the storage and power demands placed on batteries have increased, the associated materials systems have evolved. However, cost reduction and performance improvements are still necessary to address future energy storage requirements. These limitations can be overcome only by major advances in new materials needed for sustainability; providing energy independence for both present and future generations. Lithium ion cells continue to be a promising source of energy for portable applications in the future [1–4]. Many of these new applications of lithium ion batteries require high energy and power densities, quick recharging times, and safe operation at variable ambient temperatures. Typically, intercalated lithium compounds such as $LiCoO_2$, $LiMn_2O_4$, $LiFePO_4$, LiC_6 and $Li_4Ti_5O_{12}$ are the preferred electrodes in such cells [4–9]. The preparation and electrochemical performance of lithium titanate ($Li_4Ti_5O_{12}$) is of special interest due to the potentially greater safety associated with its use as an anode material.

Nanostructured electrodes offer a tremendous potential for developing high power density lithium ion batteries with high rate capabilities. The advantages of nanostructured electrodes are (i) A large amount of Li^+ is found at surfaces because the surface area/weight ratio is very large for nanoparticles. Thus, diffusion reactions occur mostly near the particle surface without relying on slow solid-state diffusion of Li^+ within the bulk. This facilitates rapid charge-discharge. (ii) Since the important electrochemical reactions occur mostly in the surface regions of particles, stress-induced lattice deformation from repeated charge/discharge is minimized. This improves cycle life and coulomb efficiency. (iii) The path length for solid-state diffusion is small as the particle diameter (d) is greatly decreased. This dramatically reduces intercalation/de-intercalation time ($t \sim [d^2/D]$ where t = intercalation/deintercalation time, d = particle/grain diameter, and D = the diffusion coefficient). (iv) Nanoparticles provide a large interface area for Li^+ insertion/extraction and hence increase the specific capacity. (v) At high C-rates, current density increases and slow Li^+ transport causes concentration polarization within the active material, preventing full utilization of the capacity. This problem is minimized for nanoparticles since active surface area increases

*To whom correspondence should be addressed:
Email: lannuttj@matsceng.ohio-state.edu
Phone: (O): 614-292-3926, Fax. (O): 614-292-1537

(current density decreases) and mass transport becomes faster (reduced diffusion length).

Last few decades have seen an effort in designing three-dimensional (3D) architectures for electrodes in Li batteries to maximize energy and power density [10–11]. Various approaches such as micromachining or templating have been investigated to design stable electrodes for lithium batteries [12–15]. 3D architectures provide high surface area to volume ratios and continuous networks and thus promise decreased system weight for increased portability as well as multiple pathways for enhanced ionic and electronic diffusion. Li et al. have shown the utility of electrospinning for designing 3D electrodes with uniaxially aligned arrays of ceramic nanofibers [16]. Similarly, Lu et al. demonstrated the stability of $Li_4Ti_5O_{12}$ electrode even after insertion of Li ions when patterned electrodes are designed [17]. Electrospinning provides a simple, inexpensive technique that can be used to fabricate electrodes composed of nano-diameter fibers [16]. This process does not require either large equipment or elaborate materials preparation and significant quantities can be electrospun to act as electrodes in a cell. Faster diffusion within such electrodes can be achieved by improving ionic and electronic diffusion within the electrodes as well as faster charge transfer across the interfaces within the components of a cell. To boost intra-electrode diffusion, nano-size grains in an electrode can promote both faster grain boundary as well as intra-granular diffusion [18]. For greater charge transfer across different components of the cell, high surface and contact areas need to be achieved. Both of these requirements can be potentially achieved by electrospinning nano-diameter fibers with high specific surface areas. This manuscript reports initial work conducted to investigate both, the process of potentially fabricating nano-diameter $Li_4Ti_5O_{12}$ fibers; and their electrochemical performance as anode for lithium ion batteries.

2. EXPERIMENTAL

Two spin dopes with different wt % compositions in the range 4 – 5 wt % LTO + PVP in isopropanol were utilized. First, a mixture of lithium and titanium oxide nanoparticles dispersed in isopropanol was obtained from Metamateria Technologies (Columbus, OH). PVP (polyvinylpyrolidone, Sigma-Aldrich, 360,000 MW) was dissolved in isopropanol at 5 wt % and this solution added to the lithium and titanium nanoparticle solutions by gentle stirring at ~50°C. Excess solvent was removed by evaporation in a Rotovap (Buchi Rotovapor RE 121) to produce concentrated LTO + PVP nanoparticle solutions typically containing approximately 5% PVP. X-ray diffraction (XRD, Rigaku Ultima III) was used to characterize the crystal structure of LTO powder after heat treating the colloid and pyrolyzing at 700°C for 4 hours in ambient atmosphere.

Both solutions were electrospun using a voltage of 15 – 17 kV during extrusion from a syringe onto a metallic target (on aluminum foil wrapping a steel plate) at a distance of 20 cm. The flow rates were varied from 0.1 – 3 mLh^{-1}. The optimal composition was also electrospun under low humidity (20% RH) conditions in a plastic enclosure. To explore the effects of temperature, they were spun onto a target maintained at higher temperature (≥120˚C) and into a high temperature ambient atmosphere (>100˚C) maintained using a heat lamp. Electrospun samples were then pyrolyzed at 600 and 700˚C for 2 hours at a heating rate of 2˚Cm^{-1} in ambient atmosphere (air) in a high temperature Carbolite CWF 1200 furnace.

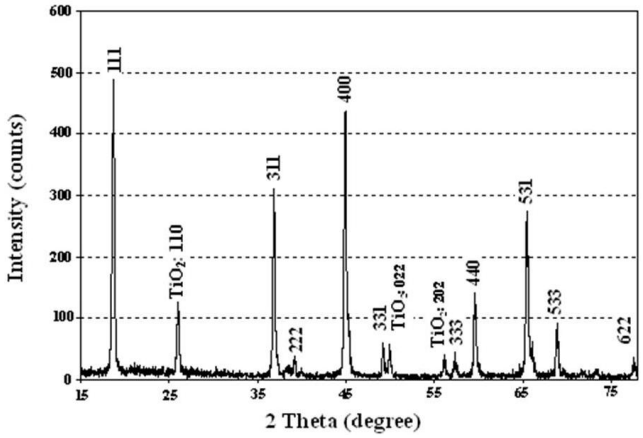

Figure 1. XRD pattern of LTO powder obtained from the LTO colloid used for electrospinning.

Fibers pyrolyzed at 700˚C were then plasma treated in the presence of oxygen under a pressure of 500 mTorr for 30 minutes to activate the local LTO crystallites within the pyrolyzed fiber and clean the sample by removing carbon-based impurities [20]. The fibers were examined using a Sirion high-resolution field-emission gun scanning electron microscope (SEM) at specific stages to determine their morphology. Electrodes were prepared for measuring electrochemical performance by mixing 95 wt % LTO and 5 wt % polytetrafluoroethylene (PTFE) (Aldrich) or polyvinylidine fluoride (PVDF) (Aldrich) as a binder. The mixture was rolled into thin sheets and circular electrodes of area ~0.64 cm^2 were fabricated . Conductive carbon powder was added to provide required electronic conductivity. The electrodes typically had an active material (LTO) content of ~ 8 mg. The electrodes were then tested against metallic lithium in a stainless steel coin cell containing electrolyte, a polypropylene separator, and a current collector. Electrolyte was prepared by adding 1 M $LiClO_4$ in 1:1:1 (by volume) ethylene carbonate (EC) + diethyl carbonate (DEC) + dimethyl carbonate (DMC). The anode and cathode caps of the coin cells were then crimped together with a polypropylene gasket in-between. Cyclic performance of the coin cells was evaluated using a Parstat 2273 potentiostat with voltage ranging from 1 to 2.5 V. A $Li \| Li_4Ti_5O_{12}$ cell was fabricated and electrochemical measurements conducted to determine the capacities, charge – discharge characteristics, and performance at different C rates.

3. RESULTS AND DISCUSSION

Figure 1 shows the XRD pattern obtained from a typical colloid precursor used for electrospinning. The XRD pattern matched the standard for lithium titanate ($Li_4Ti_5O_{12}$). However, a few peaks were observed that seemed to be derived from secondary phases such as TiO_2. This may be due to TiO_2 colloid aggregates present when the precursor is processed. Figures 2 (a – b) are representative SEM images of electrospun fibers from two different compositions. Substantial beading can be observed in the fiber sheet electrospun from the 4 wt % LTO + PVP composition [Figure 2 (a)]. Beading occurred when the wt % was relatively low regardless of adjustments to electrospinning parameters (15 – 25 kV and flow

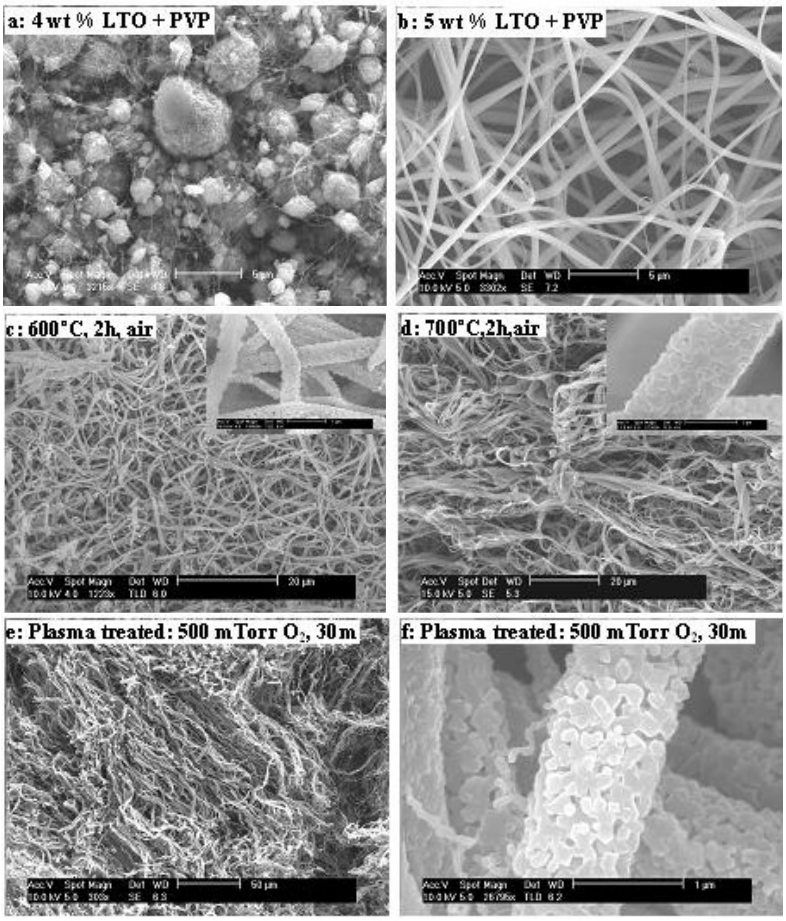

Figure 2. SEM images of LTO fiber samples electrospun from different compositions (a & b), after pyrolysis (c & d), and subsequent plasma treatment (e & f).

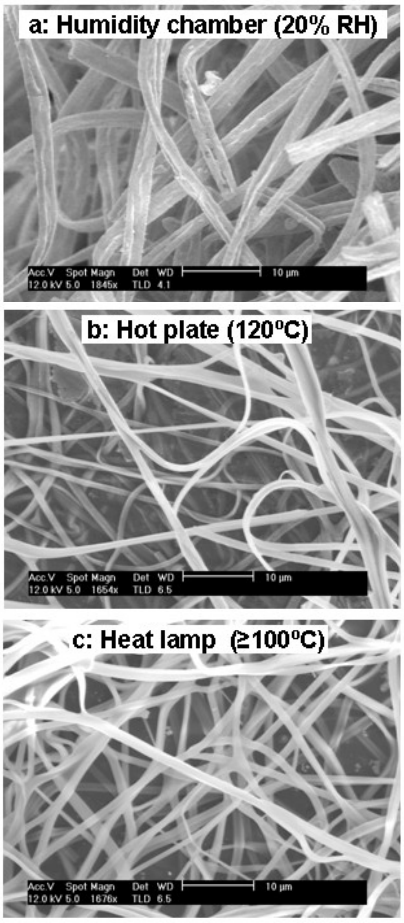

Figure 3. SEM images of LTO fiber samples electrospun in various ambient conditions.

rates of 0.1 – 5 mlh^{-1}). However, the 5 wt % LTO + PVP composition [Figure 2 (b)] spun at 15 kV and a flow rate of 3 mlh^{-1} was found to result in bead-free, submicron fiber. The mean fiber diameter of the fiber spun was 414 ± 99 nm. Hence, all further experiments were conducted on the higher wt % composition. Figures 2 (c – d) are the SEM images of the same fibers pyrolyzed at 600 and 700˚C for 2 hours in air. Higher magnifications of the pyrolyzed fibers are visible in the insets. Individual nano-sized LTO crystallites can be seen in pyrolyzed fibers at higher magnification, especially those pyrolyzed at 700˚C. Energy dispersion x-ray spectroscopy (EDS) revealed only Ti and O peaks. Thus, 700˚C for 2 hours in air proved to be appropriate conditions to pyrolyze PVP and completely expose the nano-grained lithium titanate to conceivably enhance diffusion. Figures 2 (e – f) are SEM images at different magnifications of a 700˚C pyrolyzed sample plasma-treated in oxygen for 30 minutes. This further cleaned up the fiber and exposed the LTO crystallites/grains within the individual fibers. The grain size of the crystallites was 111 ± 30 nm. Such smaller grains can boost the ionic diffusion within the grains. At the same time, electronic diffusion along the grain boundary should be enhanced due to increased grain boundary surface area.

In another set of experiments, the solution was electrospun in controlled humidity conditions. Ambient humidity during electrospinning can vary from very low (25% RH) to very high (≥ 75% RH) depending on seasonal conditions. PVP - based electrospinning compositions have been observed to plasticize into a film within minutes at high humidities [19], thus destroying the nanofiber structure. Although, the electrospun LTO fibers seem to be able to withstand high humidity for longer periods compared to LMO and TNBT precursors [18 – 19], they could potentially become plasticized over longer time periods. Hence, three different approaches were investigated. The first approach was to spin LTO fibers in controlled humidity. This was achieved by electrospinning the precursor in a plastic enclosure (plastic box) into which nitrogen could be added to reduce and maintain humidity to ≤20% [18]. The second approach was to electrospin LTO fibers directly on to a high temperature target (≥120˚C) at ambient humidities ≥50%. The third approach was to electrospin LTO fibers in the presence of a heat lamp. The purpose was to provide a high temperature (>100˚C) exposure from the tip of the Taylor cone to the target while the LTO solution is being spun to eliminate moisture sensitivity by thermally cross-linking the PVP.

Figures 3 (a – c) are the SEM images of the fibers electrospun using these approaches. Figure 3 (a) is a SEM image of the LTO

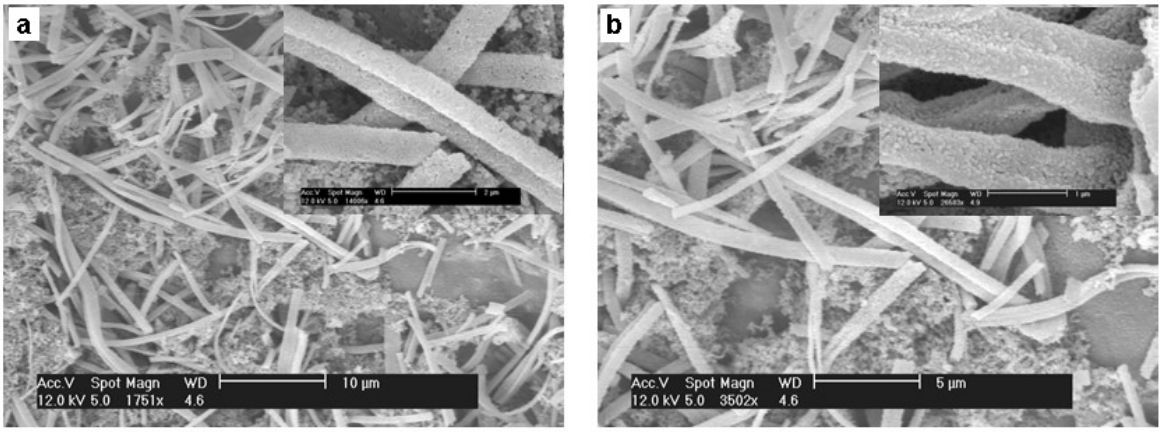

Figure 4. SEM images of LTO anodes (Insets are high magnification SEM images).

fibers spun in the humidity chamber at ~ 20% RH. While a few fibers display cracking along their length, majority of the fibers were contiguous and interconnected within the sheet. Fibers spun either directly onto a hot target [Figure 3(b)] or in hot ambient atmospheres [Figure 3(c)] were pristine, contiguous and completely inter-connected. This is advantageous as these contiguous, interconnected fibers could act as channels along which electrons diffuse during its application as an anode. Thus, these fibers show promise as electrodes with better ionic and electronic pathways for faster diffusion in an electrochemical cell. Fibers emerging from two different process conditions were examined for surface area. Table 1 shows the measured BET surface area of as-spun fibers on a target at room temperature and at elevated temperature (>120˚C). This indicates that the fibers spun at higher temperatures experience increase in surface due to evaporation of the PVP at these temperatures. Electrospinning onto a hot target appeared to increase the surface area by almost 80% suggesting that such fibers could provide more atomic sites for ion exchange and enhance diffusion.

Figures 4 (a – b) are the SEM images of 700˚C pyrolyzed LTO anodes used for testing. Insets show high magnification images of the same anode in which nano-size LTO crystallites are clearly visible. Not surprisingly, LTO ceramic fibers tend to be fragile and continuity may have been lost when they were mixed with active C fiber during anode fabrication. Figure 5 is a plot of three consecutive charge-discharge cycles from a Li‖$Li_4Ti_5O_{12}$ coin cell. The curves were generated by applying constant current in the voltage range of 1 – 2.5 V. The anode seems to have reasonable capacity compared to theoretical capacity with very little degradation observed in all three curves .Thus, it seems that the capacity retention is close to 100% after three charge – discharge cycles. However, in comparison to the capacity retention of ≥90% retention observed by

Table 1. Measured surface area of LTO fibers electrospun using different conditions.

Type of material	Surface area ($m^2.g^{-1}$)
LTO fibers (Humidity chamber)	4.9
LTO fibers (Hot plate ~120˚C)	8.8

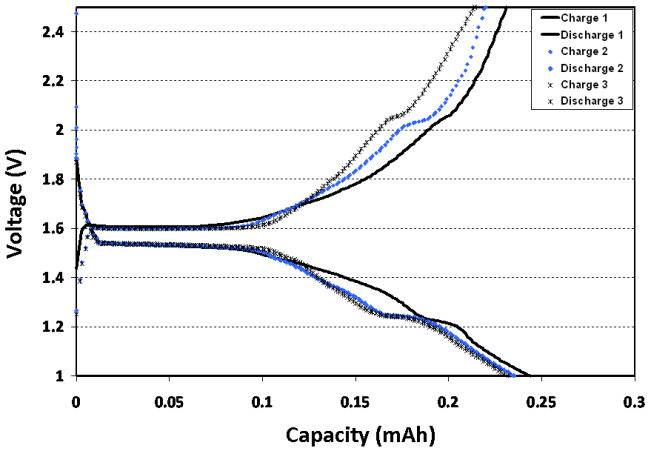

Figure 5. Charge-discharge capacity of LTO anodes during three consecutive cycles.

Belharouak et al. [22] over 1000 cycles, it is possible that the cells may experience higher loss in capacity. Figures 6 (a – b) show the cyclic voltammograms (CV) of $Li_4Ti_5O_{12}$ obtained at different scanning rates of 0.1 and 0.25 mVs^{-1}. At both the scanning rates, a pair of reversible redox peaks can be clearly seen that correspond to the cathodic and anodic processes. The cathodic peak located around 1.50V at 0.1mVs^{-1} corresponds to the voltage plateau of the first cycle discharge process in which Li intercalates into the spinel $Li_4Ti_5O_{12}$ and moves steadily to lower voltage with increasing scanning rate. The anodic peak located at 1.66V corresponds to the voltage plateau of the first cycle charge process in which Li deintercalates from the spinel $Li_{4+x}Ti_5O_{12}$ and moves steadily to the higher voltage with increasing scanning rate. Moreover, there is a small peak among the cathodic and anodic peaks at higher scanning rates (0.25 mVs^{-1}) indicating the presence of secondary impurity phases. X-ray fluorescence indicated the presence of iron and silicon in small quantities within the fibers. The first pair of cathodic and anodic peaks correspond to intercalation/deintercalation of Li in the range $1 \leq x \leq 0.5$ and the second pair corresponds to intercalation/deintercalation of Li in the range $0.5 \leq x \leq 0$. Typically, this

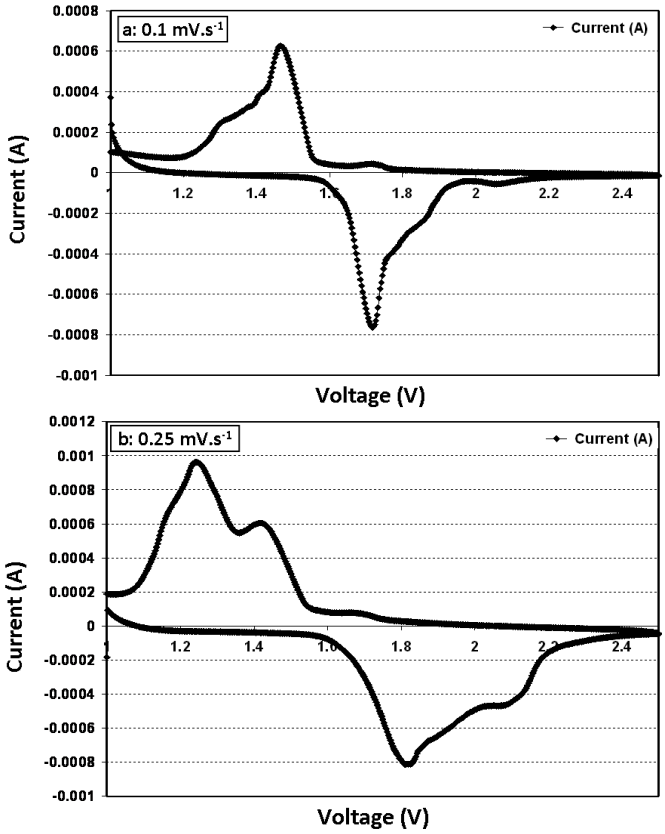

Figure 6. CV curves from coin cells at a scanning rate of (a) 0.1 mVs^{-1} and (b) 0.25 mVs^{-1}.

is attributed to the removal/addition of Li ions from/into half of the tetrahedral sites in which Li/Li interaction occurs while the second pair occurs due to this process at the other tetrahedral sites where Li/Li intercalations do not exist [23 – 24]. Chen et al. [25] observed a solid state diffusion-controlled process for lithium ions with diffusion coefficients of the order of $10^{-11} – 10^{-12}$ $cm^2.s^{-1}$. In comparison, the diffusion coefficients in our anodes seem to be an order of magnitude lower. This could potentially be due to the impurities present in the anode as well as interparticle contact that could provide shorter pathways for diffusion and needs further investigation.

Coin cells were also prepared from the same batch of fibers to study the effects of different C rates. During testing, each cycle comprises one charge and one discharge curve at constant current. The current required to complete one charge cycle from 3 to 4.2 V in one hour is called the "1C" rate [21]. If it took only half an hour to complete one charge cycle it is designated as "2C," and if the cycle was completed in two hours it is designated as "C/2." In our experiment, charging was always performed at C/5 rate and discharge rates were varied from C/5 to 20C. The percentage values of charge and discharge capacities of LTO fibers are shown in the Figure 7. The discharge capacities were > 80% when charged up to a rate of 5C, but 50% loss was observed at higher C rates (20C). Potential presence of secondary phases such as TiO_2, Fe_2O_3 and SiO_2, lack of contiguity and interconnectivity of the fibers within the anode, and degradation during continuous charging could result

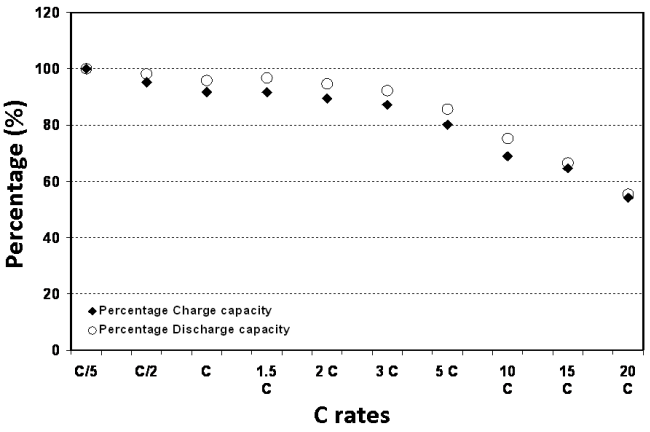

Figure 7. Charge discharge capacities for the coin cell prepared from LTO fibers as a function of rate of discharging.

in loss of capacities when charging at higher rates. Hence, it seems beneficial to use precursors (raw materials) that have lower impurity content to prepare the electrospinning solution. Additionally, careful handling and processing is required to maintain the contiguous fiber structure within the anode during its fabrication. To improve the charging speeds and the charge generated, faster transfer of Li ions from the $Li_4Ti_5O_{12}$ is desirable. This may be possible by using appropriate dopants that promote faster intercalation and deintercalation of Li ions to and from the $Li_4Ti_5O_{12}$ spinel [26 – 30].

4. CONCLUSIONS

High specific surface area lithium titanate ($Li_4Ti_5O_{12}$) anodes comprised of submicron fibers with nanosize grains were fabricated for potential applications in lithium ion batteries. Appropriate precursor compositions allowed electrospinning to produce submicron fibers comprised of nanosize grains. Different techniques were examined to avoid plasticization caused due to ambient humidity. Electrospinning in low humidity or in a high temperature atmosphere resulted in a pristine fiber mat that could be easily handled for subsequent processing. Pyrolyzing the fibers at 700˚C for 2 hours in ambient conditions and plasma treating in O_2 atmosphere for 30 minutes was found to be optimal to maintain fiber structure and expose nano-scale LTO crystallites. Electrochemical testing resulted in comparable performance with no losses for three charge-discharge cycles. CV curves resulted in peaks at cathodic and anodic potentials indicating intercalation and deintercalation of Li in and out of the $Li_4Ti_5O_{12}$ spinel. Also, a small peak was observed when charged at higher scanning rate (0.25 mVs^{-1}) indicating presence of secondary impurities, which may be present in the precursor materials or formed during processing. The capacity generated was competitive with ≥ 80% capacity reached at rates of C/5 to 10C. Further work should also include investigation of aligned electrospun $Li_4Ti_5O_{12}$ fibers as these can provide shortest pathways for ionic and electronic diffusion and thus spur diffusion within the anode. Addition of dopants can also boost ionic diffusivity and the intercalation of Li ions into the $Li_4Ti_5O_{12}$ spinel and thus the electrochemical performance of the anode.

5. ACKNOWLEDGEMENTS

This material is based upon work supported by the National Science Foundation Grant Nos. IIP-0930626 and EEC-0425626. Any opinions, findings, and conclusions or recommendations expressed in this material are those of the authors and do not reflect the views of the National Science Foundation.

REFERENCES

[1] W.J. Zhang, J. Power Sources, 196, 13 (2011).
[2] U. Kasavajjula, C.S. Wang, A.J. Appleby, J. Power Sources, 163, 1003 (2007).
[3] C.M. Park, J.H. Kim, H. Kim, H.J. Sohn, Chem. Soc. Rev., 39, 3115 (2010).
[4] J.M. Tarascon, M. Armand, Nature, 414, 359 (2001).
[5] S.Y. Chung, J.T. Bloking, Y.M. Chang, Nature Materials, 1, 123 (2002).
[6] A. Yamada, S.C. Chung, K. Hinokuma, J. Electrochemical Society, 148, A224 (2001).
[7] J.W. Fergus, J. Power Sources, 195, 939 (2010).
[8] H.W. Lu, L. Yu, W. Zeng, Y.S. Li, Z. W. Fu, Electrochemical and Solid-State Letters, 11, A140 (2008).
[9] Z.W. Fu, J. Ma, Q.Z. Qin, Solid State Ionics, 176, 1635 (2005).
[10]J.W. Long, B. Dunn, D.R. Rolison, H.S. White, Chemical Reviews, 104, 4463 (2004).
[11]R.W. Hart, H.S. White, B. Dunn, D.R. Rolison, Electrochemistry Communications, 5, 120 (2003).
[12]C.L. Wang, L. Taherabadi, G.Y. Jia, M. Madou, Y.T. Yeh, B. Dunn, Eletrochemical & Solid-State Letters, 7, A435 (2004).
[13]Baure G, Kown C, Lee G, Chamran F, Kim C, Dunn B, Micropower and Microdevices, v. PV 2002-25, The Electrochem. Soc. Proc. Series, Pennington, NJ, 2003.
[14]J.C. Lytle, H.W. Yan, N.S. Ergang, W.H. Smyrl, A. Stein, J. Mater. Chem., 14, 1616 (2004).
[15]A. Stein, R.C. Schroden, Solid State and Materials Science, 5, 553 (2001).
[16]D. Li, Y.N. Xia, Nano Letters, 3, 555 (2003).
[17]H.W. Lu, W. Zeng, Y.S. Li, Z.W. Fu, J. Power Sources, 164, 874 (2007).
[18]Tikekar N., Lannutti J., Revur R., Sengupta S., Unpublished results.
[19]Tikekar N., & Lannutti J., Ceramics Interntional, in press.
[20]C.C. Chen, K.-F. Chiu, K.M. Lin, H.C. Lin, C.-R. Yang, F.M. Wang, Physica Scripta, T129, 74 (2007).
[21]P. Poizot, S. Laruelle, S. Grugeon, L. Dupont, J.M. Tarascon, Nature, 407, 499 (2000).
[22]I. Belharouak, G. Koenig Jr., K. Amine, J. Power Sources, 196, 10344 (2011).
[23]N. Sinha, N. Minuchandraiah, J. Solid State Electrochem., 12, 1619 (2008).
[24]B. Hwang, R. Santhanam, D. Liu, J. Power Sources, 97, 443 (2001).
[25]J. Chen, L. Yang, S. Fang, S. Hirano, K. Tachibana, J. Power Sources, 200, 59 (2012).
[26]B. Tian, H. Xiang, L. Zhang, H. Wang, J. Solid State Electrochemistry, 16, 205 (2012).
[27]K. Mukai, K. Ariyoshi, T. Ohzuku, J. Power Sources, 146, 213 (2005).
[28]H. Zhao, Y. Li, Z. Zhu, J. Lin, Z. Tian, R, Wang, Electrochimica Acta, 53, 7079 (2008).
[29]J. Wolfenstine, J. Allen, J. Power Sources, 180, 582 (2008).
[30]M. Ganesan, Ionics, 14, 395 (2008).